Journal of Power Sources, 46 (1993) 219–230

PbO_2 active material as an electrocrystalline network

E. Bashtavelova and A. Winsel
Universität Gesamthochschule Kassel, 35321 Kassel (Germany)

Abstract

According to the 'agglomerate-of-spheres' (AOS) model the PbO_2 electrode is considered as an electrocrystalline network of agglomerates of interconnected small particles with a common surface. Its electrical and mechanical properties are determined by the behaviour of the narrow contact zones ('necks'). Therefore, the apparent electronic conductivity of the PbO_2 network is the effective sensor for the behaviour of the necks. In order to achieve a better understanding of the PbO_2 electrode by direct measuring the physical characteristics, which are involved in the AOS model, we have developed a new type of experiment and the corresponding equipment. It consists of a special electrochemical cell integrated into a tension-testing machine. It enables us to cycle the positive electrode and to measure simultaneously the resistance between the grid and the active material, as well as the apparent conductivity of the electrocrystalline PbO_2 network during formation, charge and discharge. The registration of the resistance and of the force (strength) during the formation process allows us to observe the creation of the AOS structure at the very first time, when the mechanic and electronic connections are formed, that is immediately after the current is switched on. Then a negative force is generated. We call this force 'electroformative'. It is associated with the expansion of the PbO_2 electrode as a cause of the formation of the ball-like AOS structure. The registration of the same parameters during charge and discharge shows, that the increase of the solid-state resistance of the PbO_2 limits the discharge capacity of the positive electrode. But during discharge one can observe a decrease of the resistance at the beginning; the discharge process proceeds at lower values, until the resistance increases rapidly at the end of discharge. This is in accordance with the AOS model. This states that the apparent conductance of the electrocrystalline network is governed by the constriction resistances of the neck regions and not so much by the volume of the spheres. But the necks do also determine the strength of the PbO_2 network. Therefore, after cycling of the electrode, a rupture process is performed and the electronic resistance, the force (strength), and the dilatation are registered simultaneously again. The results enable us to obtain the tensile strength of the necks.

Introduction

According to the 'agglomerate-of-spheres' model (the AOS model) [1, 2], the electrical and mechanical properties of the electrocrystalline network of the PbO_2 active material are determined by the behaviour of the narrow contact zones between the particles. These ones are called 'necks'. In order to achieve a better understanding of the PbO_2 electrode new types of experiments and corresponding equipment have been developed for the *in situ* measurement of the physical characteristics that are involved in the AOS model.

0378-7753/93/$6.00

Experimental

Setup

The experimental setup consists of a special electrochemical cell with integrated tension testing equipment. It allows automatic and simultaneous monitoring of the following parameters: current, electrode potential versus hydrogen electrode, solid-state resistance, and strength (the force applied to the rod). Figure 1 presents a schematic design and Fig. 2 a photograph of the electrochemical cell.

The force is registered by means of a special sensor. The resistance is measured with direct-current according to the so-called 'four-point' method.

At the beginning of the experiment, the lead rod is pressed slightly on a tablet of unformed paste. The latter is pasted into a lead mould and constitutes the positive electrode. This electrode, together with a negative lead electrode, is placed in a Plexiglas container that is filled with sulfuric acid electrolyte. The tablet has a diameter of 20 mm and a thickness of 2 mm. The diameter of the lead rod is 8 mm.

Procedure

Experiments were performed on three different sample bodies with different sizes of contact area between the tablet and the lead mould, i.e.:

(i) bowl-like electrode: pasted tablet in a lead mould;

(ii) Corbino disc: electrode as in (i) but with an insulator sheet between the tablet and the lead mould;

(iii) side-area-free tablet situated between rod and mould.

In order to evaluate the influence of the resistance of the grid/active-material interface, two separate components have been introduced into the total resistance, W, namely: (i) material resistance $W_m = \hat{o}d/F$; (ii) interface resistance $W_s = \kappa/F_1 + \kappa/F_2$. Furthermore, d is the thickness of the tablet, $W = W_M + W_s$. F_1 and F_2 are the interfacial areas of the contacts. According to geometrical calculations, the three different sample bodies behave as follows:

(i) bowl-like electrode:
material resistance $W_m = 0.1131\hat{o}$
interface resistance $W_s = 2.2780\kappa$

(ii) Corbino disc:
material resistance $W_m = 0.6982\hat{o}$
interface resistance $W_s = 2.6782\kappa$

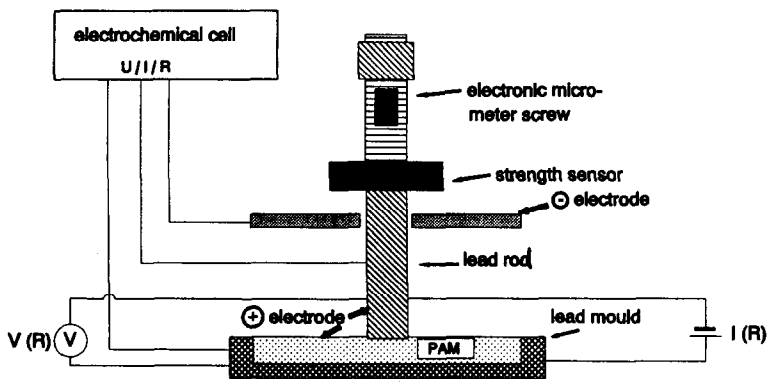

Fig. 1. Schematic design of electrochemical cell.

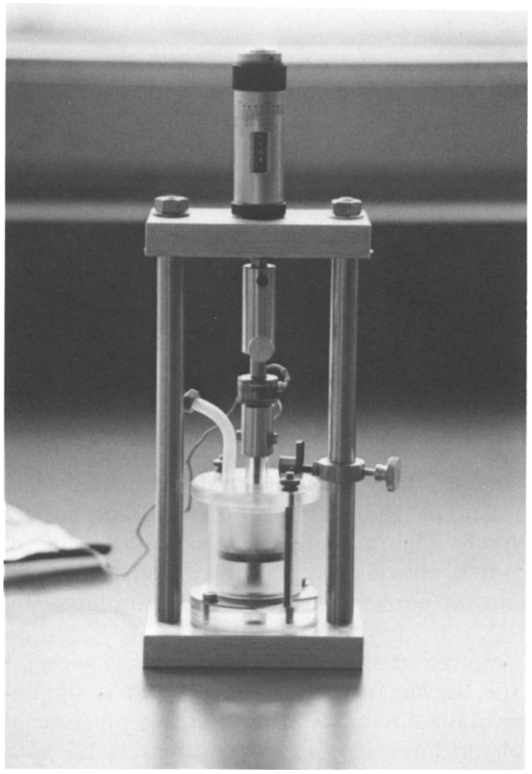

Fig. 2. Photograph of electrochemical cell.

(iii) free situated tablet:

material resistance $W_m = 0.2155\hat{o}$

interface resistance $W_s = 2.5705\kappa$

where κ is the apparent area-specific interface resistance of the boundary lead/PbO_2; $\hat{o}$ is the apparent specific resistance of the lead dioxide active material.

The equipment allows the positive electrode to be formed and cycled. During these processes, a direct current is transmitted through the lead rod. In this way, the rod behaves like the grid in the positive electrode. The resistance between the rod and the active material, as well as the apparent conductivity of the electrocrystalline PbO_2 network, are measured. The internal pressure is also registered.

The simultaneous monitoring of the resistance of the PbO_2 network and of the force between the rod and the tablet during the formation and cycling processes provides an opportunity to observe simultaneously the self-organized generation of the AOS structure of PbO_2 active material when the mechanical and the electronic connections are formed.

After the cycling process, the rod is pulled up slowly with the aid of a micrometer screw. During this rupture experiment, again the electronic resistance, the force and the dilatation between rod and tablet are registered simultaneously. The tensile strength of the necks is determined because if an AOS body is torn and ruptured into two pieces, the resulting surface is the weakest plane through the body and this plane contains necks only.

Results and discussion

Variation of force and tension

Figure 3 presents the variation of the force and the resistance during formation of a bowl-like electrode with a current of 10 mA g^{-1}. As can be seen, the resistance decreases after a few hours as soon as the electronic connection between the rod and the lead mould through the growing PbO_2 bridges has been established. Later on, the formation process proceeds at a comparatively small resistance.

Immediately after the current is switched on, a negative force is generated, which acts from the bottom of the rod. This negative force is generated by the tendency of the formed PbO_2 to enlarge the entire volume of the electrode. This enlargement causes a pressure within the active material, which is proportional to the formation time. In other words, the force is almost proportional to the amount of formed PbO_2. Due to the volume balance of the formation process, a shrinking of the shaped volume of the pasted electrode is expected. Instead, an expansion of the active material is observed in all experiments.

During the formation of the free-standing tablet, the generated force is much smaller compared with that of the bowl-like electrode. This is expected, because the side-areas of the tablet can be moved freely. Figure 4 presents the variation of the force during formation with 25 mA g^{-1}. It is obvious that the force depends on the density of the formation current: the higher the current, the smaller the absolute value of the force.

This expansion indicates a volume change of the electrode. In the experiment reported here, there is an increase in the thickness of the tablet, which is situated in a lead mould and cannot move in the other directions. This causes a pressure on the rod, which is registered by means of the force sensor. Its sensitivity is 1.5 μV/p and 42.9 μV/μm. The sensitivity of the voltage measurements is 1.0 μV. The values obtained for the increase of the thickness are between 10 and 40 μm. These values are in good agreement with those that have been calculated from the experimental data of the apparent density, composition, and weight of the paste and active material.

The expansion of the porous PbO_2 structure is associated with the mechanisms prevailing during the successive generation of the PbO_2 AOS structure, and with the electromodelling forces which act at the same time.

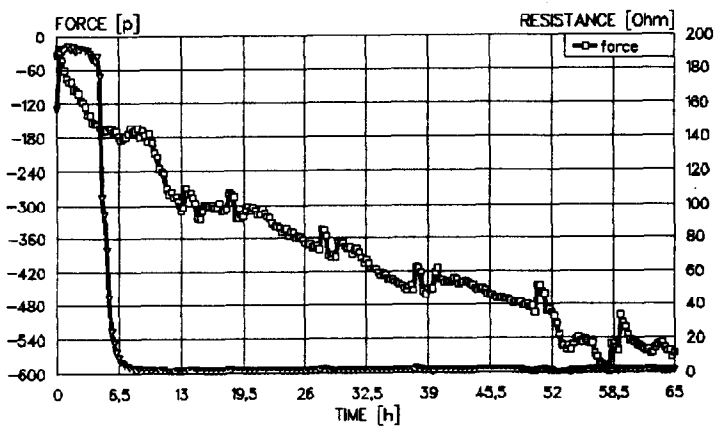

Fig. 3. Force and resistance variations during formation of a bowl-like electrode; formation 10 mA g^{-1}.

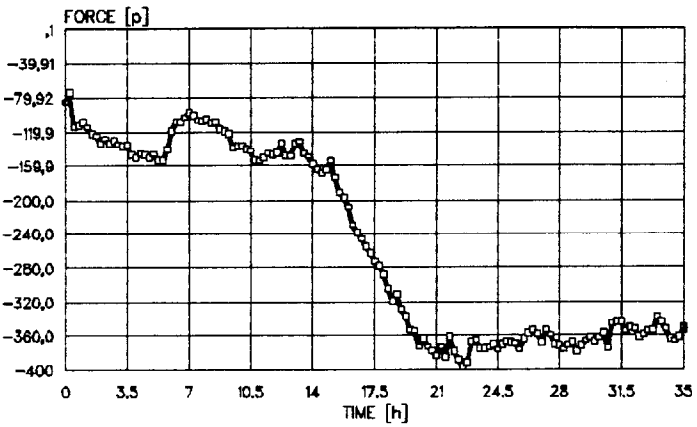

Fig. 4. Force during formation with increased current; formation 25 mA g^{-1}.

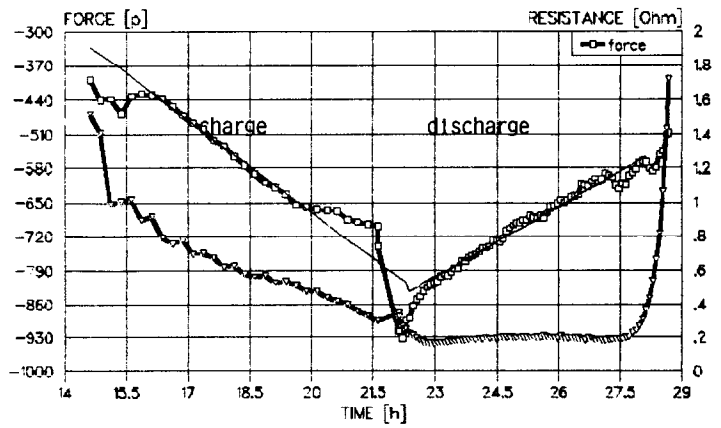

Fig. 5. Pressure force and resistance during one charge/discharge cycle.

Figure 5 presents the simultaneous measurement of the pressure force and resistance during one charge/discharge cycle. The pressure force increases during charge and decreases during discharge. At the end of discharge, the force reaches approximately the same value as at the beginning of the charge. The experimentally obtained values of the thickness decrease with discharge are $\backsim$5–10 μm. These values are in agreement with those calculated from the experimental data of the apparent density.

An electrode has been cycled and the pressure force relieved during a charge phase by pulling up the rod with the aid of the micrometer screw. Afterwards, cycling was continued. As Fig. 6 shows, the force rises again until the end of charge, and during discharge it decreases. This behaviour can be explained as follows. During discharge, the generated $PbSO_4$ is deposited within the free-pore space without stretching of the PbO_2 network. But when, during recharge, this $PbSO_4$ is reconverted to PbO_2, the electroformative forces are effective again. This is in agreement with the AOS model.

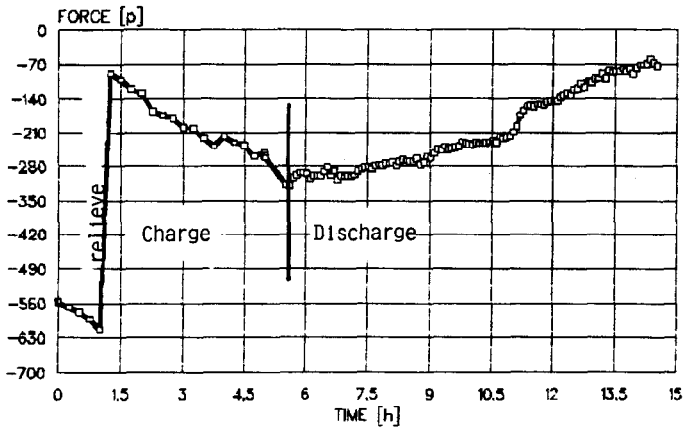

Fig. 6. Relief of force during charge.

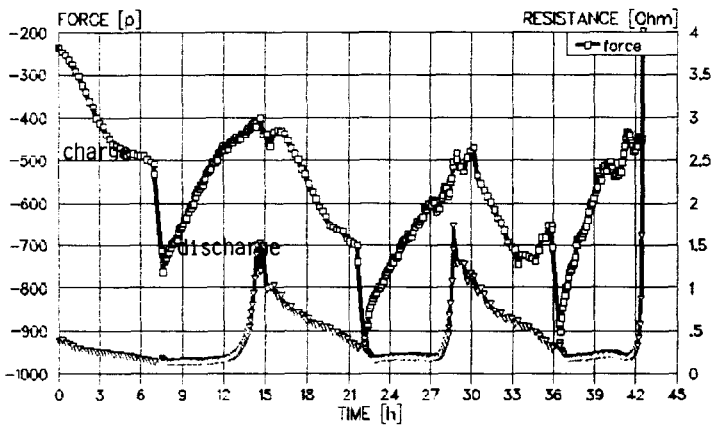

Fig. 7. Variation of tensile strength (pressure force) during three consecutive cycles.

Figure 7 presents the variation of the tensile strength (pressure force) during three consecutive cycles. It demonstrates that the electrode behaviour is uniform at any state of charge or discharge. It also confirms the fact that the pressure force increases during charge and decreases during discharge. During the first few cycles, the pressure force increases from cycle to cycle. Later, it seems to converge to a limiting value, Fig. 8. This can be explained by alterations to the structure of the active material during the initial cycles.

The finding that the volume of the charged active material is larger than the volume of the cured paste and larger than the volume of the discharged active material, is very important because it is connected directly with the stability and cycle life of the positive electrode. It is planned to investigate the conditions under which this pressure force is smallest. In other words, the conditions that influence the pressure state of the PbO_2 crystalline network and affect the electromodelling forces during the generation of the PbO_2 AOS structure.

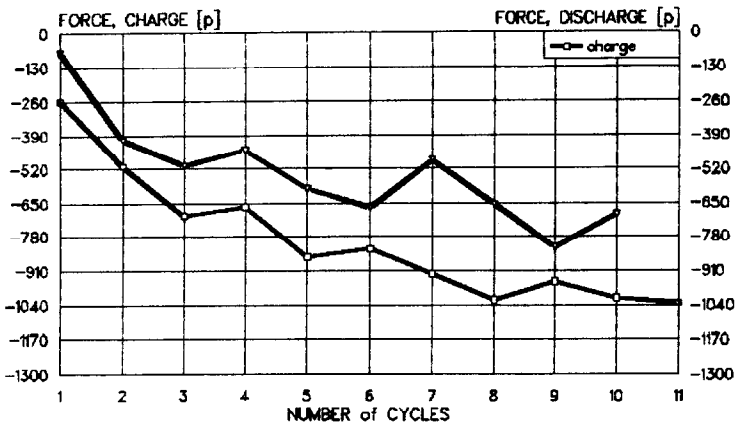

Fig. 8. Pressure force at the end of the charge and discharge period as a function of cycle number; charge/discharge 12.5 mA g^{-1}.

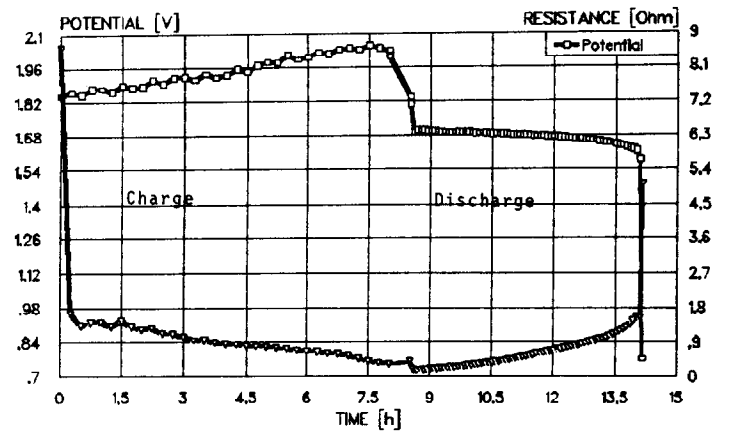

Fig. 9. Variation of resistance during one charge and discharge cycle as a function of time.

Variation of resistance during cycling

As has been shown previously [3–6], the utilization of the positive active material is determined by the resistance. But this statement requires further investigation. Figure 9 presents the variation of the resistance during one charge/discharge cycle as a function of time. During charging, except at the very beginning, the resistance decreases continuously from its large value at the end of the preceding discharge process. The sharp decrease at the beginning is associated with the formation of renewed necks by a planar nucleation process. After this, the network is reconstructed according to the AOS model.

Evidently, at the very beginning of discharge, the value of the resistance decreases to about half its value at the end of charge. Then, the resistance of the active material (solid-state resistance) decreases slightly and the discharge process proceeds at lower values compared with those during charge. At the end of discharge, the resistance increases rapidly. An explanation of this phenomenon can be derived from the following considerations.

- The amount of PbO_2, which is dissolved by discharge, does not determine the resistance of the active material. Consequently, discharge cannot occur in the neck regions
- According to the AOS model, the decrease in the resistance is connected with lowering of the apparent specific bulk resistance:

$$\hat{o} = \hat{o}^* R/h \tag{1}$$

where $\hat{o}$ is the apparent specific bulk resistance; $\hat{o}^*$ is the specific material resistance: R is the radius of the sphere; h is the radius of the neck.

This decrease can occur when: (i) the specific material resistance $\hat{o}^*$ decreases through the increasing concentration of charge carriers, possibly affected by the removal of oxygen (increase of the stoichiometric deviation δ in $PbO_{2-\delta}$); (ii) the neck radius h increases by the incorporation of lead ions from the neighbour region. The latter is to be expected since, on discharge, sufficient free-lead ions are available and the necks exhibit local potentials that are more negative than those in the regions of the spheres. This is in agreement with the AOS model.

Figure 10 presents the variation of resistance and potential during three consecutive cycles. The results again demonstrate that the electrode behaviour is uniform at any state of charge or discharge. It is also confirmed that the resistance passes through a minimum. Data for the last cycle before a change in the charge current and immediately after its reduction are given in Fig. 11. A diminution in material utilization (capacity) is evident. Using the equation $W_m = 0.1131\hat{o}$, calculations were made of the average values of the resistances for each charge and discharge cycle, and the corresponding average values of the apparent specific resistance $\hat{o}$.

The dependence between $\hat{o}$ and discharge capacity during cycling is given in Fig. 12. Again, it can be seen that the discharge capacity decreases when the average value of the apparent specific resistance, $\hat{o}$, during discharge increases.

As described above, different sample bodies were used in the experiments. This allows an assessment to be made of the partial influence of the resistance of the active material and the resistance between the active material and the grid (between tablet and rod). For this purpose, one bowl-like electrode and one Corbino disc were cycled. The difference between these electrodes was the different size of the contact area between the tablet and the lead mould. From the experimental data for the

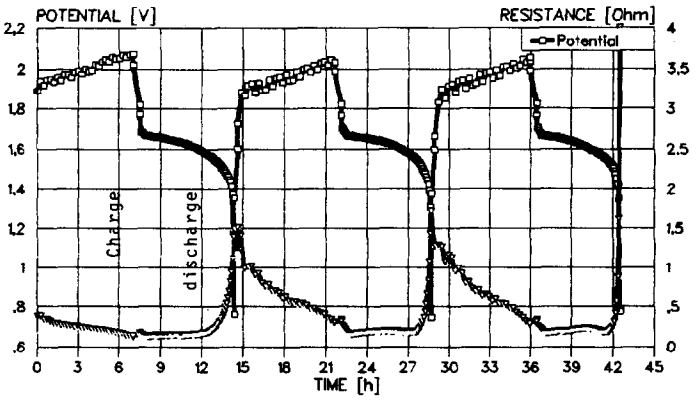

Fig. 10. Variation of resistance and potential during three consecutive cycles as a function of time.

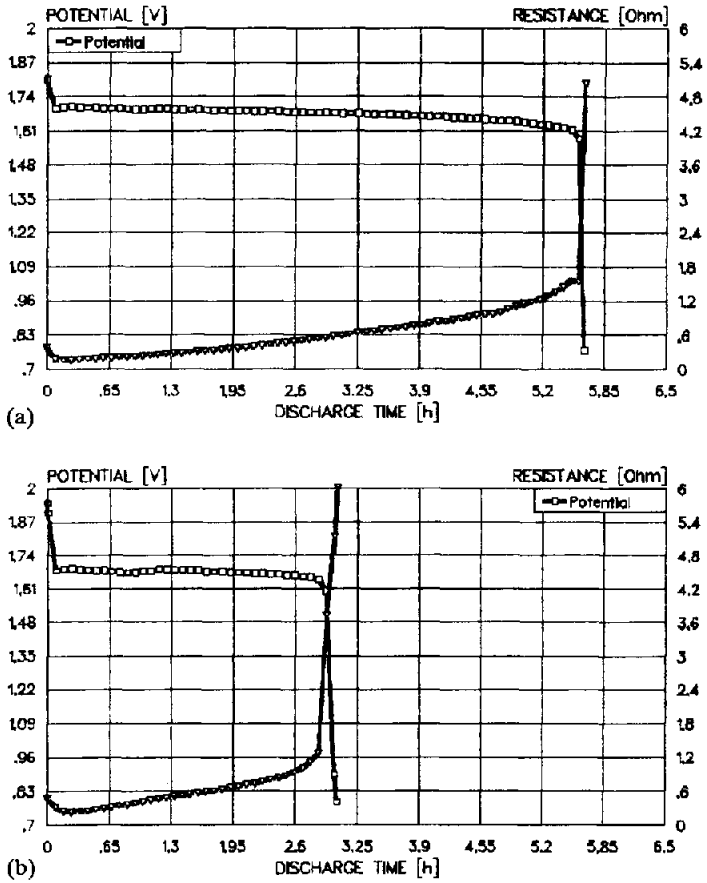

Fig. 11. Resistance and potential as a function of the discharge time before and after reduction of the charge current: (a) charge current 12.5 mA g^{-1}; (b) charge current 6 mA g^{-1}.

resistances during discharge of the two samples, the average values of the resistances for these two cases were calculated. Using the formulae discussed above, the apparent specific resistance and the apparent specific interface resistance were calculated, see Table 1.

These two resistances provide an opportunity to determine, in future experiments, the influence of different parameters on the resistance between the grid and the active material.

Strength and resistance during a rupture process

According to the AOS model, the necks determine the strength of one AOS configuration. Figure 13 presents the variation of strength, potential and resistance of a 100% charged electrode as a function of the dilatation during a stress experiment.

The maximal strength value is equivalent to the tensile strength of the necks. At this peak point at a dilatation of 0.06 mm, the resistance is growing continuously. The variation of both the resistance and the potential with respect to the dilatation indicate precisely at which point the body is ruptured into two pieces. In other words, the

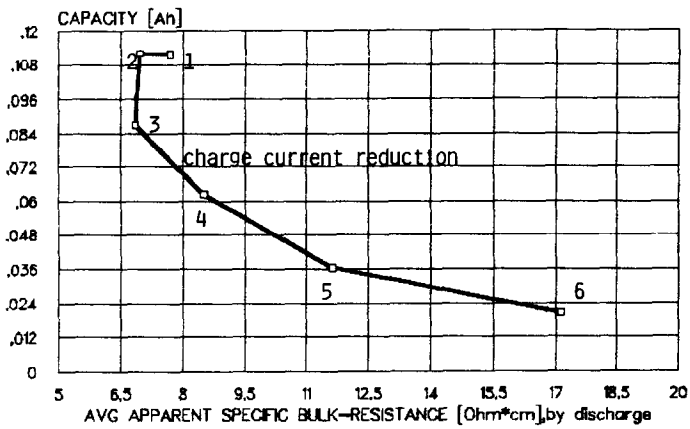

Fig. 12. Average value of the apparent specific resistance, $\hat{o}$, during discharge as a function of the capacity.

TABLE 1

Resistance data

	R (average) (Ω)	Material resistance, W_m (Ω cm)	Surface resistance, W_s (Ω cm^2)
Bowl-like electrode	0.0811	$0.1131\hat{o}$	2.2780κ
Corbino disc	0.3232	$0.6982\hat{o}$	2.6782κ
Result	$\hat{o}=0.4032$ Ω cm $\kappa=0.0156$ Ω cm^2		

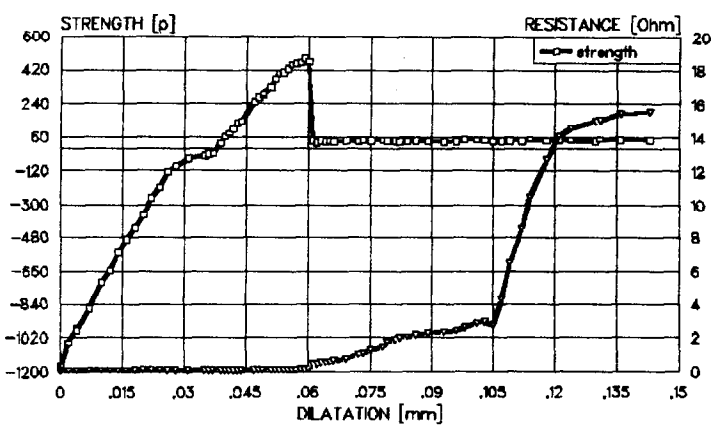

Fig. 13. Variation of strength, potential and resistance of a 100%-charged electrode as a function of the dilatation during the stress experiment.

rupture occurs when both the resistance and the potential begin to increase rapidly. In this case, a direct current flows through an electrolysis cell which is formed by the two separated pieces of the body. It appears that the voltage relaxation is accelerated when stress is exerted on a PbO_2 electrode.

After the stress experiment just described, the ruptured parts were put together again, pressed with the previous highest pressure force, and then ruptured again. The strength and resistance during this procedure is shown in Fig. 14. Three important results can be derived from this diagram:

(i) a tensile strength is no longer observable;

(ii) the initial resistance is increased;

(iii) the dilatation range up to the increase of resistance is smaller.

The explanation for this behaviour is as follows. The necks, which have been formed under the action of the electroformative forces and which have been ruptured in the first stress experiment, have not been restored again under the applied pressure or are too small to be stable, when the pressure force is reduced during the second stress experiment.

Evidently, the tensile strength data allow the average radius of the necks to be calculated. The traction force is defined as a positive mechanical force:

$$\epsilon = F/A \tag{2}$$

where F is the necessary tensile strength; A is the total rupture plain.

In the present case, $A = \Sigma S_h$ is the total surface area of all necks. According to Gmelin, the tensile strength of PbO_2 is: $\epsilon = (3 \pm 2)10^5$ g cm^{-3}. From eqn. (2) it follows that:

$$\epsilon = F/\Sigma S_h \tag{3}$$

and,

$$h = \sqrt{(F/\pi \epsilon n)} \tag{4}$$

where h is the average radius of the necks, $h = \sqrt{(S_h/\pi)}$; n is the total number of all necks on the rupture plane.

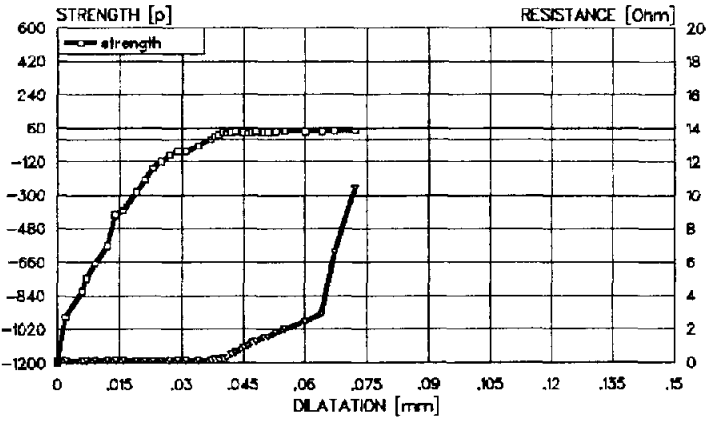

Fig. 14. Strength and resistance as a function of dilatation during second rupture procedure.

This number was evaluated by counting the peaks of ball-like particles of the ruptured plane with the aid of special stereo SEM photography. The average radius, R, of the particles (spheres) was determined in the same way.

In the present case, $n = 0.0527 \times 10^8$; $F = 515$ p (the experimental value of the tensile strength); $R = 0.48$ μm (average radius of the spheres). With these values, a value of 0.15 μm is obtained for the neck radius and 3.2 for the R/h ratio.

The critical value of this ratio, which determines the minimum neck radius, has been calculated by Winsel and Voss [1], using the δ values of Pohl and Rickert [7]. The critical value is $R/h \leqslant 5.9$.

Consequently, the two different methods of R/h determination are delivering nearly the same results.

Acknowledgements

The authors are indebted to Mr K.-H. Otto and Mr H. Sauer for their help during the construction of the cell and other equipment. The work has been partly supported by the 'Herbert-Quandt-Stiftung' of VARTA AG and by ILZRO Inc. Thanks are also due to the board of VARTA AG, and to Dr E. Voss for many discussions.

References

1 A. Winsel, E. Voss and U. Hullmeine, *DECHEMA-Monogr., 121* (1990) 209–231.
2 A. Winsel, E. Voss and U. Hullmeine, *J. Power Sources, 30* (1990) 209–226.
3 W. Borger, U. Hullmeine, H. Laig-Hörstebrock and E. Meißner, in T. Keily and B.W. Baxter (eds.), *Power Sources 12, Research and Development in Non-Mechanical Electric Power Sources,* International Power Sources Symposium Committee, Leatherhead, UK, 1989, pp. 131–144.
4 M. Calabek, K. Micka, in K. Bullock and D. Pavlov (eds.), *Proc. Symp. on Advances in Lead/Acid Batteries, New Orleans, LA, USA,* Vol. 84-14, The Electrochemical Society, Pennington, NJ, USA, 1984, pp. 288–301.
5 M. Calabek, K. Micka and J. Sandera, *J. Power Sources, 10* (1983) 271.
6 M. Calabek and M. Micka, *Electrochim. Acta, 37* (1992) 1805.
7 J.P. Pohl and H. Rickert, in S. Trasatti (ed.), *Electrodes of Conductive Metallic Oxides,* Elsevier, Amsterdam, 1980, pp. 183–220.